International Journal of Mechanical Engineering (IJME)
ISSN(P): 2319-2240; ISSN(E): 2319-2259
Vol. 3, Issue 4, July 2014, 35-48
© IASET

International Academy of Science, Engineering and Technology
Connecting Researchers; Nurturing Innovations

EFFECT OF REFLUX ON PERISTALTIC MOTION IN AN ASYMMETRIC CHANNEL WITH PARTIAL SLIP AND DIFFERENT WAVE FORMS

P. SRINIVASA RAO[1] & G. BHANODAYA REDDY[2]

Department of Mechanical Engineering, Sri Venkateswara University, Tirupati, Andhra Pradesh, India

ABSTRACT

In this paper, the partial slip effect and impact of different wave forms are discussed on the peristaltic flow of a Newtonian fluid in an asymmetric channel. The channel asymmetry is produced by choosing a peristaltic wave train on the wall with different amplitudes and phases. Mathematical analysis has been carried out for small Reynolds number and long wavelength. The solutions for stream function, axial velocity and pressure gradient are obtained. Numerical integration has been performed for the pumping, frictional forces, trapping and reflux phenomena. It is observed that the pumping against pressure rise, axial velocity, pressure gradient, size of the trapped bolus and reflux layer decrease with increasing the partial slip parameter. The size of the bolus symmetry disappears for large value of the partial slip parameter. Under certain conditions, there are boluses of fluid moving at the speed as if they were trapped by the wave. The comparison among the different wave forms (namely triangular, sinusoidal, trapezoidal and square) in the fluid flow indicates that the square wave yields largest flux.

KEYWORDS: Peristaltic Transport, Partial Slip, Pumping, Trapping, Reflux and Different Wave Forms

INTRODUCTION

Peristaltic flow plays a vital role in a living body. This mechanism is responsible for a form of fluid transport induced by a progressive wave of area contraction or expansion along the length of a distensible tube/channel containing fluid. The type of fluid transport process is motivated because its importance in small intestine, gastro-intestine tract, mobility of stomach, cervical canal, passage of urine from kidney to bladder through ureter, the transport of food bolus through the esophagus, food mixing, transport of spermatozoa in cervical canal, movement of eggs in the female fallopian tube, the moment of chyme in small intestine and many others. Also, peristaltic transport occurs in many practical applications involving biomechanical systems such as roller and finger pumps. Such a wide occurrence of peristaltic motion should not be surprising all since it results physiologically from neuro-muscular properties of any tubular smooth muscle.

Study in peristalsis has been presented by Latham [1]. Earliest then Jaffrin and shaprio [2] and Jaffrin [3] investigated the peristaltic transport in channel. The mathematical models obtained by train of periodic sinusoidal waves in an infinity long two-dimensional symmetric or asymmetric channel containing fluid have been investigated in [4-11] and many others. Many of these models explain the basic fluid mechanics aspects of peristalsis, namely the characteristic of pumping, trapping and reflux. These models are developed in two ways, one by restricting to small peristaltic wave amplitude with arbitrary Reynolds number and the other by lubrication theory in which the fluid inertia and wall curvature are neglected without any restriction on amplitude.

The flow analysis in channel with partial slip is well recognized field of investigation due to its occurrence in biomedical Engineering for example in the dialysis of blood in artificial kidney, preservation of food, gaseous diffusion, in transpiration cooling boundary layer control in the flow of blood in the capillaries and for the flow in blood oxygenators. The dynamic interaction of flexible boundary with fluid in peristaltic motion is important from mechanical point of view**.** Beavers and Joseph [12] introduced the concept of partial slip. The slip at the wall is presented through a condition formulated by Saffman [13] which can be viewed as an improved version of the condition by the Beavers and Joseph. Recent literatures on the peristaltic motion with considerations of the nature of the fluid, geometry of the tube/channel, propagating waves and asymmetry are found in [14-22]**.**

The aim of the present study is to investigate the peristaltic transport in a two-dimensional asymmetric channel under the effect of partial slip. The channel asymmetry is generated by choosing the peristaltic wave train on the walls to have different amplitude and phase due to the variation in channel width, wave amplitude and phase differences with different wave forms as introduced by Hayat *et al* [23]. In addition to reproducing the earlier results, we clearly bring out the significance of the pumping characteristics, velocity distribution, pressure gradient, trapping and reflux. The non-dimensional expressions for the different wave forms are considered for pumping and trapping phenomena. The comparison among the four wave forms is carefully analyzed.

Mathematical Formulation and Solution

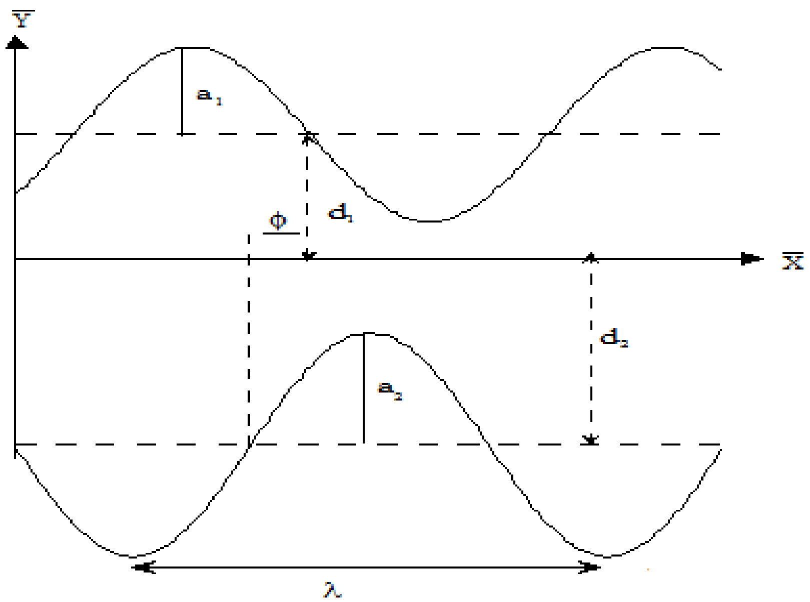

Figure 1: Schematic Diagram of a Two-Dimensional Asymmetric Channel

We consider the motion of an incompressible viscous fluid in a two-dimensional channel (Figure 1). The sinusoidal wave trains propagating with constant speed c along the channel walls are

$$\bar{Y} = H_1 = \bar{d}_1 + \bar{a}_1 \cos\left[\frac{2\pi}{\lambda}\left(\bar{X} - c\bar{t}\right)\right] \text{……….upper wall,} \quad (1)$$

$$\bar{Y} = H_2 = -\bar{d}_2 - \bar{b}_1 \cos\left[\frac{2\pi}{\lambda}(\bar{X} - c\bar{t}) + \phi\right] \text{……lower wall.} \quad (2)$$

where $\bar{a}_1$ and $\bar{b}_1$ are the amplitudes of the waves, λ is the wave length, $\bar{d}_1 + \bar{d}_2$ is the width of the channel, *c* is the velocity of propagation, $\bar{t}$ is the time and $\bar{X}$ is the direction of wave propagation. The phase difference ϕ varies in the range $0 \le \phi \le \pi$ in which $\phi = 0$ corresponds to symmetric channel with waves out of phase and $\phi = \pi$ the waves are in phase. Further $\bar{a}_1$, $\bar{b}_1$, $\bar{d}_1$, $\bar{d}_2$ and ϕ satisfy the condition $\bar{a}_1^2 + \bar{b}_1^2 + 2\bar{a}_1\bar{b}_1\cos\phi \le (\bar{d}_1 + \bar{d}_2)^2$.

The governing equations of motion are given by

$$\frac{\partial \bar{U}}{\partial \bar{X}} + \frac{\partial \bar{V}}{\partial \bar{Y}} = 0, \tag{3}$$

$$\frac{\partial \bar{U}}{\partial \bar{t}} + \bar{U}\frac{\partial \bar{U}}{\partial \bar{X}} + \bar{V}\frac{\partial \bar{U}}{\partial \bar{Y}} = -\frac{1}{\rho}\frac{\partial \bar{P}}{\partial \bar{X}} + v\left(\frac{\partial^2 \bar{U}}{\partial \bar{X}^2} + \frac{\partial^2 \bar{U}}{\partial \bar{Y}^2}\right), \tag{4}$$

$$\frac{\partial \bar{V}}{\partial \bar{t}} + \bar{U}\frac{\partial \bar{V}}{\partial \bar{X}} + \bar{V}\frac{\partial \bar{V}}{\partial \bar{Y}} = -\frac{1}{\rho}\frac{\partial \bar{P}}{\partial \bar{Y}} + v\left(\frac{\partial^2 \bar{V}}{\partial \bar{X}^2} + \frac{\partial^2 \bar{V}}{\partial \bar{Y}^2}\right), \tag{5}$$

Where $\bar{U}$ and $\bar{V}$ are the respective velocity components in the $\bar{X}$ and $\bar{Y}$ directions in the fixed frame, $\bar{P}$ is the fluid pressure, ρ is the constant density of the fluid and v is the kinematic viscosity. We introduce a wave frame $(\bar{x}, \bar{y})$ moving with velocity c away from the fixed frame $(\bar{X}, \bar{Y})$ by the transformations

$$\bar{x} = \bar{X} - c\bar{t}, \bar{y} = \bar{Y}, \bar{u} = \bar{U} - c, \ \bar{v} = \bar{V}, \quad \bar{p}(x) = \bar{P}(X,t). \tag{6}$$

The appropriate non-dimensional variables and parameters are defined as

$$x = \frac{\bar{x}}{\lambda}, y = \frac{\bar{y}}{\bar{d}_1}, \ u = \frac{\bar{u}}{c}, \ v = \frac{\bar{v}}{c}, \ h_1 = \frac{\bar{H}_1}{\bar{d}_1}, \ h_2 = \frac{\bar{H}_2}{\bar{d}_2}, \quad t = \frac{c}{\lambda}\bar{t}, \ a = \frac{\bar{a}_1}{\bar{d}_1}, \ b = \frac{\bar{b}_1}{\bar{d}_1}, \ d = \frac{\bar{d}_2}{\bar{d}_1},$$

$$\delta = \frac{\bar{d}_1}{\lambda}, \ v = \frac{\bar{V}}{c\delta}, \ R_e = \frac{c\bar{d}_1}{v}, \ \psi = \frac{\bar{\psi}}{c\bar{d}_1}, \ Da = \frac{k}{d_1^2}.$$

Using the above non-dimensional variables and parameters Eqs. (3) - (5) in terms of stream function $\psi\left(u = \frac{\partial \psi}{\partial y}, v = -\delta\frac{\partial \psi}{\partial x}\right)$ is given by

$$R_e\delta\left\{\psi_y\psi_{yyx} - \psi_x\psi_{yyy} + \delta^2\left(\psi_y\psi_{xxx} - \psi_x\psi_{xxy}\right)\right\} = \psi_{yyyy} + 2\delta^2\psi_{xxyy} + \delta^4\psi_{xxxx}. \tag{7}$$

Here and in what follows the subscripts x and y denote the partial differentiations.

The corresponding boundary conditions in terms of stream function ψ are defined as

$$\psi = \frac{q}{2} \ at \ y = h_1(x), \tag{8}$$

$$\psi = \frac{-q}{2} \ at \ y = h_2(x), \tag{9}$$

$$\frac{\partial\psi}{\partial y}+\beta\frac{\partial^2\psi}{\partial y^2}=-1\ at\ y=h_1(x), \tag{10}$$

$$\frac{\partial\psi}{\partial y}-\beta\frac{\partial^2\psi}{\partial y^2}=-1\ at\ y=h_2(x), \tag{11}$$

Where β is a slip parameter, with $h_1(x)=1+a\cos 2\pi x$, and $h_2(x)=-d-b\cos(2\pi x+\phi)$, q is the flux in fixed frame and a, b, d and ϕ satisfy the relation $a^2+b^2+2ab\cos\phi\le(1+d)^2$.

Under the assumptions of the long wavelength $\delta<<1$ and low Reynolds number, the Eq. (7) becomes

$$\psi_{yyyy}=0. \tag{12}$$

The solution of Eq. (12) satisfying the corresponding boundary conditions (8) to (11) is

$$\psi=\frac{(q+h_1-h_2)}{(h_1-h_2)^2(h_1-h_2-6\beta)}\left(2y^3-3(h_1+h_2)y^2-6(h_1-h_2-h_1h_2)y+6\beta h_1(h_1-h_2)-h_1^3+3h_1^2h_2\right)+\frac{q}{2}+h_1-y, \tag{13}$$

In order to check the result obtained above, it can be observed from Eq. (13) that as β → 0, the expression of the stream function reduces to that obtained by Ebaid in [9] at zero magnetic parameter. The axial velocity component can be calculated by differentiating (13) w.r.to y and given as

$$u=\frac{6(q+h_1-h_2)}{(h_1-h_2)^2(h_2-h_1-6\beta)}\left(y^2-(h_1+h_2)y-h_1+h_2+h_1h_2\right)-1\cdot \tag{14}$$

For $h_2\le y\le h_1$ the flux at any axial station in the fixed frame is

$$Q=\int_{h_2}^{h_1}(u+1)dy=\int_{h_2}^{h_1}udy+\int_{h_2}^{h_1}dy=q+(h_1-h_2)\cdot \tag{15}$$

The average volume flow rate over one period $\left(T=\frac{\lambda}{c}\right)$ of the peristaltic wave is defined as

$$\overline{Q}=\frac{1}{T}\int_o^T(q+(h_1-h_2)dt=q+1+d\cdot \tag{16}$$

The pressure gradient is obtained from the dimensionless momentum equation for the axial velocity $\frac{dp}{dx}=\psi_{yyy}$ and substituting for ψ from (13), we get

$$\frac{dp}{dx}=\frac{12(q+h_1-h_2)}{(h_1-h_2)^2(h_2-h_1-6\beta)} \tag{17}$$

Integrating equation (17) over wavelength one obtains

$$\Delta p_L=\int_0^L\left(\frac{dp}{dx}\right)dx=p_L-p_0\cdot \tag{18}$$

The integral in (18) will be independent of time only when L is an integral multiple of λ. In this problem either we have to prescribe Δp or $\bar{Q}$ and by prescribing either Δp or $\bar{Q}$ as constants, the flow can be treated as steady. The integral in (18) is evaluated over one wavelength using the values of the integrals given in Appendix and replacing q with $\bar{Q}$ from (16). Finally are have

$$\Delta p = \frac{(q-6\beta)}{3\beta^2\sqrt{L_1}} - \frac{2q(1+d)}{\beta\sqrt[3]{L_1}} + \frac{(q-6\beta)}{3\beta^2\sqrt{L_2}} \tag{19}$$

The above expression may be rewritten as

$$\bar{Q} = \frac{3\alpha\beta\left(\beta\Delta p\sqrt{L_1} + 2\left(\sqrt{L_1}+\sqrt{L_2}\right)\right)}{\sqrt{L_2}\left(\sqrt{L_1} - 6\left(1+d\right)\right) + \sqrt[3]{L_1}} + 1 + d\,. \tag{20}$$

The results for the corresponding symmetric channel can be obtained from our results by putting $a=b$, $d=1$ and $\phi=0$. Eq. (20) reduces to Poiseuille law for a channel of straight walls when $\Delta p<0$, $a=b=0$ and for a channel with peristaltic waves with same amplitude and in phase when $a=b$ and $\phi=\pi$.

The frictional forces at y= h_1 and y= h_2 are denoted by

$$F_1 = \int_0^1 -h_1^2\left(\frac{dp}{dx}\right)dx\,, \tag{21}$$

$$F_2 = \int_0^1 -h_2^2\left(\frac{dp}{dx}\right)dx\,. \tag{22}$$

DISCUSSIONS OF THE RESULTS

Velocity Distribution and Pressure Gradient

The maximum velocity occurs at $y=\frac{h_1+h_2}{2}$. From Eq. (14) we obtain

$$u_{\max} = \frac{3\left(1+d-\bar{Q}\right)\left(h_2-h_1\right)\left(4-h_2+h_1\right)+\left(h_1-h_2\right)^2\left(12\left(\beta-1\right)-h_1+h_2\right)}{2\left(h_1-h_2\right)^2\left(h_2-h_1-6\beta\right)}\,. \tag{23}$$

The variation of the velocity u with y is computed from Eq. (14) for different values of β and $\bar{Q}$ in Figure 2 for three different cases when the amplitude of the peristaltic wave on the upper and lower walls is same $a=0.5$, $b=0.5$, channel width $d=1$ and phase shift $\phi=\pi/3$. In Figure 2(a) for $\bar{Q}=1$, it is observed that the velocity u decreases with increasing the slip parameter β. Figure 2(b) shows the variation of velocity u for various mean flux $\bar{Q}$ when $\beta=0.1$. We also noted that the velocity u increases with increasing the mean flux $\bar{Q}$. The variation of the pressure gradient dp/dx with x is calculated from Eq. (17) for different values of partial slip β and mean flux $\bar{Q}$ with $a=0.5$, $b=0.5$, $\phi=\pi/6$ and $d=1$, this is depicted in Figure 3. Figure 3(a) displays the result of the slip parameter β when $\bar{Q}=1$. We observed that the pressure gradient dp/dx decreases with increasing β . Moreover the pressure gradient decreases when we go from the nonporous case to the porous one. The effect of the mean flux $\bar{Q}$ is drawn in Figure 3(b) when $\beta = 0.1$. It can be seen that the pressure gradient increases with decrease in mean flux $\bar{Q}$.

Pumping Characteristics

The characteristic feature of a peristaltic motion is pumping against pressure rise.

At $\bar{Q} = 0$, we note from Eq. (20) that

$$\Delta p_{max} = \frac{-(1+d)\left(\sqrt{L_2}\left(\sqrt{L_1} - 6(1+d)\right) + \sqrt[3]{L_1}\right) - 6\alpha\beta\left(\sqrt{L_1} + \sqrt{L_2}\right)}{3\beta\sqrt[3]{L_1}}, \quad (24)$$

$$\bar{Q}_{max} = \frac{6\alpha\beta\left(\sqrt{L_1} + \sqrt{L_2}\right)}{\sqrt{L_2}\left(\sqrt{L_1} - 6(1+d)\right) + \sqrt[3]{L_1}} + 1 + d . \quad (25)$$

For $\Delta p = 0$, we have free pumping. When $\Delta p > \Delta p_{\max}$ one gets negative flux and when $\Delta p < 0$, we get $\bar{Q} > \bar{Q}_{\max}$ as the pressure assists the flow which is known as co-pumping. The complete occlusion occurs when $a^2 + b^2 + 2ab\cos\phi = (1+d)^2$ and in the case the fluid is pumped as a positive displacement pump with $\bar{Q} = 1 + d$.

Figure 4 depicts the variation of the dimensionless pressure rise ΔP_λ versus the variation of time-average flux $\bar{Q}$ is computed from Eq. (19) for different values of β and ϕ when a=0.5, b=0.5 and d=1. The graph is sectored so that the quadrant (I) designated as region the peristaltic pumping ($\bar{Q} > 0$ and $\Delta P_\lambda > 0$). Quadrant (II) is denoted the augmented flow when $\bar{Q} > 0$ wet $\Delta P_\lambda < 0$. Quadrant (IV) such that $\bar{Q} < 0$ and $\Delta P_\lambda > 0$ is called retrograde (or) backward pumping. Figure 4(a) is presented to explore the effect of β on pressure rise Δp with time-average flux $\bar{Q}$ when $\phi = \pi/3$. It is clear that the peristaltic pumping rate decreases with increasing the values of the slip parameter β and also opposite behavior in backward pumping. Figure 4(b) depicted the variation of ϕ on Δp with $\bar{Q}$ when $\beta = 0.1$. It is noted that an increases in the phase difference ϕ results to decrease in the peristaltic pumping rate.

The variation of time-average flux $\bar{Q}$ with the width of the channel d (Figure 5) is calculated from Eq. (20) for fixed a=0.9, b=0.5, $\phi = \pi/3$ and $\beta = 0.1$, is presented in Figure 5(a) for different values of Δp and it is observed that for Δp the flux rate increases when the distance d between the walls decrease. For Δp , $\bar{Q}$ increases for some d in the beginning but it starts decreasing for large d , this is because the poiseuille flow due to pressure loss dominates the peristaltic flow. The variation of time-average flux $\bar{Q}$ as a function $\bar{\phi} = \phi/\pi$, (normalized phase difference), is calculated from Eq. (20) for different values of Δp and presented in Figure 5(b) when a=0.5, b=0.5, d=1 and $\beta = 0.1$. We observe that when $\bar{\phi} = 0$, $\bar{Q}$ is maximum and it decreases as $\bar{\phi}$ increases, for $\Delta p > \Delta p_{\max}$, even for $\bar{\phi} = 0$. When $\Delta p = 0$ for (free pumping case), we observe that $\bar{Q}$ is zero for some $\bar{\phi}$ when peristaltic wave are in phase, the cross section of the channel is same through out. The results of Mishra [5] agree with our results described above. In Figure 6 investigated the square wave has given great result compare with triangular, sinusoidal and trapezoidal wave in the pressure gradient.

Tapping Criterion

It has been shown in [3] that under certain conditions, the streamlines $\psi = 0$ at the central line split to enclose a bolus of fluid particles circulating along closed streamline. This bolus moves at the wave velocity and therefore appears to be trapped by the wave. A criterion for the presence of trapping is the existence of stagnation points in the wave frame which are located at the intersection of the curve $\psi = 0$ and the central line.

The axial velocity component at the centre line is obtained by setting $y = 0$ in the Eq. (14) and the stagnation points are given by

$$u(x,0) = \frac{6\left(1+d-\bar{Q}+h_1(x)-h_2(x)\right)\left(h_1(x)-h_2(x)+h_1(x)h_2(x)\right)+\left(h_1(x)-h_2(x)\right)^3-6\beta\left(h_1(x)-h_2(x)\right)^2}{\left(h_1(x)-h_2(x)\right)^2\left(h_2(x)-h_1(x)-6\beta\right)}. \tag{26}$$

The steam lines are plotted for the amplitude of the peristaltic wave on the upper and lower walls when $a = 0.5$, $b=0.5$ and $d = 1$. The effect of stream lines for the mean flux $\bar{Q}$ is plotted in Figure 7 when $\phi = 0$ and $\beta = 0.1$. It is observed that the size of the trapping bolus increases with increasing the mean flux $\bar{Q}$. Figure 8 shows the variation of different values of slip parameter β with $\phi = 0$ and $\bar{Q}=1.5$. It is noted that the area of trapping bolus decreases with increasing β $(0 \le \beta \le 0.1)$ and bolus disappears for $\beta = 0.1$. The effect of the phase shift ϕ $(0 \le \phi \le \pi)$ is drawn in Figure 9 when $\beta = 0.1$ and $\bar{Q} = 1.5$. We found that the volume of the trapping bolus appearing at the central region for $\phi=0$ moves towards left and it decreases as ϕ increases. Further the bolus disappears at $\phi = \pi$.

Reflux Criterion

It has been shown in the studies [3, 5] that under certain condition the fluid particles near the walls have a mean speed of advance opposite to the main flow. This phenomenon may explain the ureteral reflux named after the observation that bacteria sometimes travel from the bladder to the kidneys in opposite direction to the main urine flow.

$$\frac{\bar{Q}}{\bar{Q}_{max}} = \frac{3\alpha\beta\left(\beta\Delta p\sqrt{L_1}+2\left(\sqrt{L_1}+\sqrt{L_2}\right)\right)+(1+d)\left(\sqrt{L_2}\left(\sqrt{L_1}-6(1+d)\right)+\sqrt[3]{L_1}\right)}{6\alpha\beta\left(\sqrt{L_1}+\sqrt{L_2}\right)+(1+d)\left(\sqrt{L_2}\left(\sqrt{L_1}-6(1+d)\right)+\sqrt[3]{L_1}\right)}. \tag{27}$$

The relation between $Q/\bar{Q}_{max}$ with the slip parameter β is depicted in Figure 10 for different values of the phase shift ϕ with $a = 0.5$, $b = 0.5$, $d = 1$ and $\Delta p = 0.6$. We observed that the reflux zone exists near the upper wall and the reflux layers and also trapping region increases with increasing ϕ. The variation of $Q/\bar{Q}_{max}$ with channel width d is plotted in Figure 11 for different pressure rise Δp with $a = 0.5$, b=0.5, $\phi = \pi/6$ and $\beta = 0.1$. We note that the reflux zone is formed near the upper wall for $\Delta p < 0$, while it is formed near the lower one for $\Delta p > 0$ and the trapping in the lower wall occurs for $\Delta p < 0$, while for the upper wall occurs for $\Delta p > 0$ and also neither trapping nor reflux occurs for $\Delta p = 0$. The effect of trapping and reflex layers increase in the upper wall when ($\Delta p < 0$) and decreases in the lower wall when ($\Delta p > 0$) by increasing the pressure rise Δp respectively. Form Figure 12, the variation on $Q/\bar{Q}_{max}$ with the phase shift ϕ for different values of the slip parameter β with $a = 0.5$, b=0.5, $d = 0.5$ and $\Delta p = 0.5$. It is concluded that the reflux zone exists near the lower wall, trapping occurs near the upper wall and also reflux layers and trapping increase with increasing β.

CONCLUSIONS

A mathematical model for the peristaltic transport of a Newtonian fluid in an asymmetric channel bounded by partial slip is presented. The important fluid mechanics phenomena of peristaltic transport, the axial velocity, pressure gradient, the pumping characteristics, the trapping, the variation of averaged flux with pressure rise and different wave forms as functions of the asymmetric motility parameters are discussed with the help of a simple analytic solution. The method followed here is different form earlier methods due to Jaffrin [3] and Mishra [5]. The results obtained by us agree with their results. More the effects due to partial slip arising through different wave forms are studied with ease through our analysis. The rigid wall gives more rates of flux and bigger trapping zone and reflux layer than the partial slip. The square wave form has other wave forms. Thus it is hoped that the present analysis may be used with confidence to describe the flow in roller pumps and in the gastro-intestinal tract with proper geometric modification.

APPENDIX

$$\int_0^{2\pi} \frac{d\theta}{\alpha+\beta\cos\theta+\gamma\sin\theta} = \frac{2\pi}{\sqrt{\alpha^2-\beta^2-\gamma^2}}, \ \alpha > \sqrt{\beta^2+\gamma^2}$$

$$\int_0^{2\pi} \frac{d\theta}{\left(\alpha+\beta\cos\theta+\gamma\sin\theta\right)^2} = \frac{2\pi\alpha}{\left(\alpha^2-\beta^2-\gamma^2\right)^{\frac{3}{2}}},$$

$$\int_0^{2\pi} \frac{d\theta}{\left(\alpha+\beta\cos\theta+\gamma\sin\theta\right)^3} = \frac{\pi\left(2\alpha^2+\beta^2+\gamma^2\right)}{\left(\alpha^2-\beta^2-\gamma^2\right)^{\frac{5}{2}}},$$

$$L_1 = (1+d)^2 - (a^2+b^2+2ab\cos\phi),$$

$$L_2 = (1+d+6\beta)^2 - (a^2+b^2+2ab\cos\phi),$$

Definition of Wave Shapes

The non-dimensional expressions of the considered wave forms are given by the following equations:

- Sinusoidal Wave

$$h_1(x) = 1 + a\sin(2\pi x),$$

$$h_2(x) = -d - b\sin(2\pi x + \phi).$$

- Triangular Wave

$$h_1(x) = 1 + a\left\{\frac{8}{\pi^3}\sum_{m=1}^{\infty}\frac{(-1)^{m+1}}{(2m-1)^2}\sin[(2m-1)x]\right\},$$

$$h_2\left(x\right)=-d-b\left\{\frac{8}{\pi^3}\sum_{m=1}^{\infty}\frac{(-1)^{m+1}}{(2m-1)^2}\sin[(2m-1)x+\phi]\right\}.$$

- Square Wave

$$h_1(x)=1+a\left\{\frac{4}{\pi}\sum_{m=1}^{\infty}\frac{(-1)^{m+1}}{(2m-1)}\cos\left[(2m-1)x\right]\right\},$$

$$h_2(x)=-d-b\left\{\frac{4}{\pi}\sum_{m=1}^{\infty}\frac{(-1)^{m+1}}{(2m-1)}\cos\left[(2m-1)x+\phi\right]\right\}.$$

- Trapezoidal Wave

$$h_1\left(x\right)=1+a\left\{\frac{32}{\pi^2}\sum_{m=1}^{\infty}\frac{\sin\frac{\pi}{8}(2m-1)}{(2m-1)^2}\sin[(2m-1)x]\right\},$$

$$h_2\left(x\right)=-d-b\left\{\frac{32}{\pi^2}\sum_{m=1}^{\infty}\frac{\sin\frac{\pi}{8}(2m-1)}{(2m-1)^2}\sin[(2m-1)x+\phi]\right\}.$$

REFERENCES

1. T.W. Latham, Fluid motion in peristaltic pump, M.S. Thesis, MIII, Cambridge, MA, 1966.
2. M.Y. Jaffrin, A.H. shapiro, Peristaltic pumping, Ann, Riv. Fluid Mech. 3(1971) 13-36.
3. Michel. Y. Jaffrin, Inertia and streamlines curvature effects on peristaltic pumping, Int. **J**. Engg. Sci., 11(1973) 681-699.
4. A.H. Shapiro, M.Y. Jaffrin, S.L. Wavelength at low Reynolds number, J. Fluid Mech. 37(1969) 799-825.
5. M. Mishra, A. Ramachardra Rao, Peristaltic transport of Newtonian fluid in an asymmetric channel, ZAMP. 54 (2003) 532-550.
6. C. Pozrikidis, A study of peristaltic flow, J. Fluid Mech. 180(1987) 515-527.
7. G. Radha krishnamacharya, Long wave length approximation to peristaltic motion of a power-law fluid. Rheol. Acta 21 (1982) 30-35.
8. Abd El-Naby Att, El-Misiery AEM, Effect of an endoscope and generalized Newtonian fluid on peristaltic motion. Appl. Math. Comput. 128(2002) 19-35.
9. A Ebaid, Effects of magnetic field and permeable wall condition on the peristaltic transport of a Newtonian fluid in asymmetric channel, Physics letters A 372(2008) 4493-4499.
10. L.M. Srivastava, V.P. Srivastava, Peristaltic transport of a non-Newtonian fluid: Applications to the vas deferens and small intestine, A.M. Biomed. Eng. 13(1985) 137-153.
11. M.V.Subba Reddy, A. Ramachandra Rao, S. Sreenadh, Peristaltic motion of a power-law fluid in an asymmetric channel, Int. J. Non-Linear Mech. 42(2007) 1153-1161.

12. G.S. Beavers, D.D. Joseph, Boundary conditions at a naturally permeable wall. J. Fluid Mech. 30 (1967) 197-207.

13. SAFFMAN, P.G., 1971, On the boundary condition at the surface of porous medium. Studies in Applied Mathematics, L. 93 (1971).

14. K.Vajravelu, S. Sreenadh, K. Hemadri Reddy and K. Murugesan, Peristaltic transport of a Casson fluid in contact with a Newtonian fluid in a circular tube with permeable wall, Int. J. fluid Mech. Res, 36(2009)244-254.

15. T. Hayat, M.V. Qureshi and Q. Hussiain, Effect of the peristaltic flow of an electrically conducting fluid in a porous space, Appl. Math. Modelling 33(2009)1862-1873.

16. EF. Elshehaway, N.T. Eldabe, A. Ebaid, Peristaltic transport in an asymmetric channel through a porous medium, Appl. Math. comput. 182(2006) 140-150.

17. M. Kothandapani, S. Srinivas, Nonlinear peristaltic transport in an inclined asymmetric channel through a porous medium, Phys. Lett. A372 (2008) 1265.

18. Kh.s. Mekhemier, Nonlinear peristaltic transport through a porous medium in an inclined planner channel. J. Porous Media, 6(2003)189.

19. J. C. Misra, S.K. Pandey, A mathematical model for esophageal Swallowing of a food-bolus, Math. Comput. Model 33(2001) 997-1009.

20. S. Nadeem, Noreen Sher Akbar, Naheeda Bibi, Sadaf Ashiq, Influence of heat and Mass transfer on peristaltic flow of a third order fluid in a diverging tube, Commun. Nonlin. Sci. Num. Simul. 15(2010) 2916-2931.

21. T.Hayat, Q. Hussian, N. Ali, Influence of partial slip on the peristaltic flow in a porous medium, Physica A 387(2008) 3399-3409.

22. Prasanna Harivaran, Seshadri, Rupek, Benerjee. Peristaltic transport of non-Newtonian fluid in a diverging tube with different wave forms, Math. Comput. Model. 48 (2008) 998-1017.

23. T. Hayat, Nasir Ali, Zaheer Abbas, Peristaltic flow of a micropoalr fluid in a channel with different wave forms. Phys. Lett. A 370(2008)331-344.

24. K. Vajravelu, S. Sreenadh, K. Rajanikanth, Changhoon Lee. Peristaltic transport of a Williamson fluid in asymmetric channels with permeable walls, Nonlinear Analysis: Real World Applications 13(2012)2804-2822.

APPENDICES

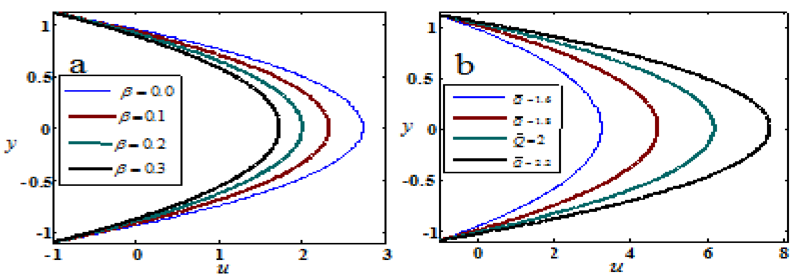

Figure 2: The Variation of u with y for A=0.5, B=0.5, D=1, $\phi=\pi/3$; A) $\bar{Q}$=1; B) $\beta=0.1$

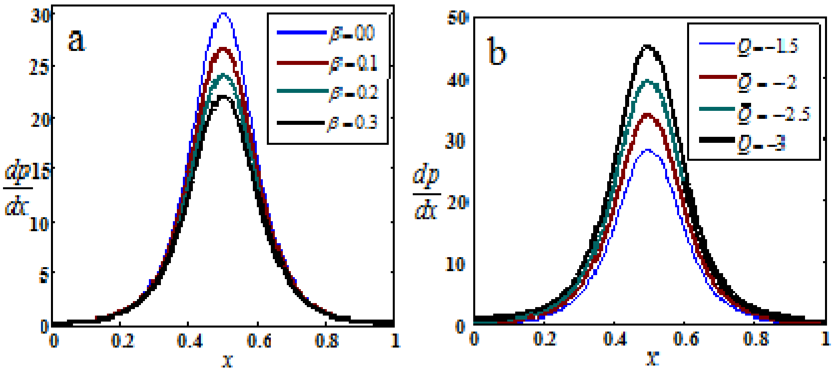

Figure 3: The Variation of $\frac{dp}{dx}$ with x for A=0.5, B=0.5, D=1; A) $\bar{Q}$=-1, B) $\beta = 0.1$

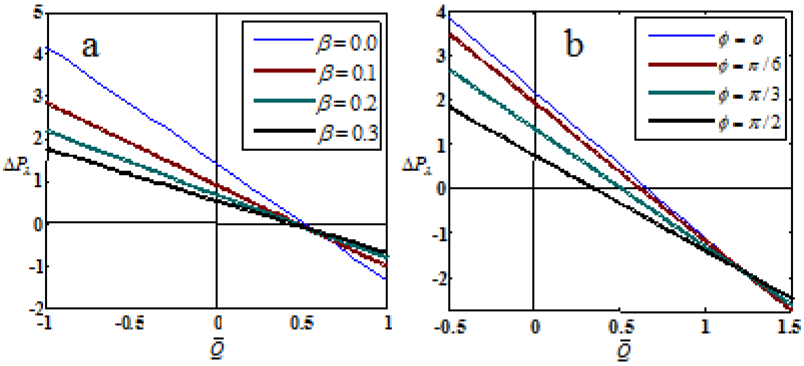

Figure 4: The Variation of Δp with $\bar{Q}$ for A=0.5, B=0.5, D=1; A) ϕ=$\pi/3$; B) $\beta = 0.1$

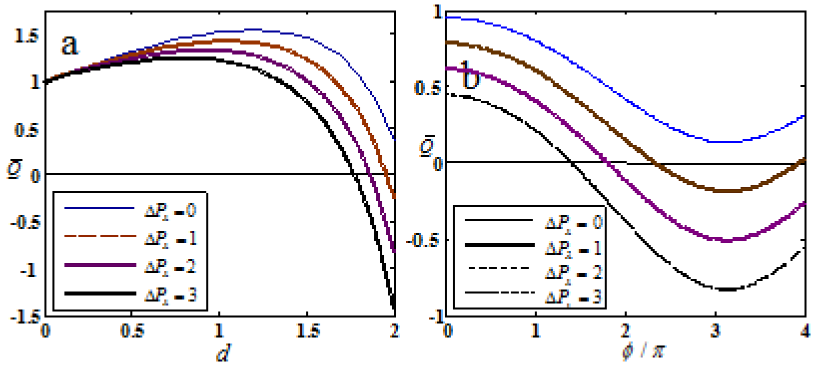

Figure 5: The Variation Of $\bar{Q}$ with d and ϕ / π for A=0.9, B=0.5; A) ϕ=$\pi/3$, $\beta = 0.1$; B) D=1, $\beta = 0.1$

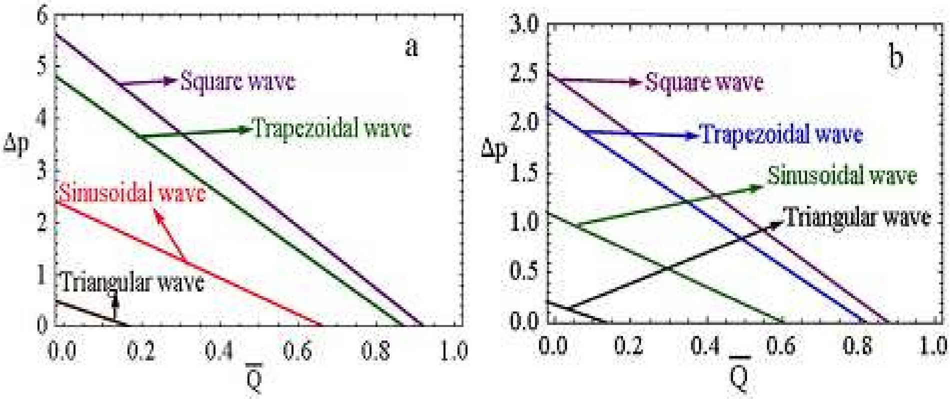

Figure 6: The Variation of Δp with $\bar{Q}$ and A=0.5, B=0.5, D=1, $\phi = 0$; A) $\beta = 0$; B) $\beta = 0.1$

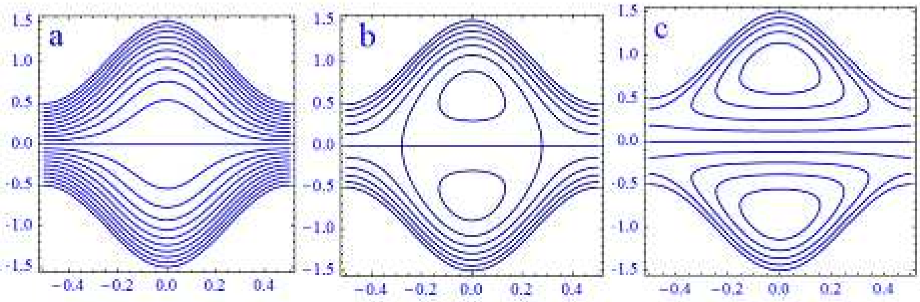

Figure 7: Streamlines for a=0.5, B=0.5, D=1, $\phi = 0$, $\beta = 0.1$ and for Different $\bar{Q}$; A) $\bar{Q}$=1; B) $\bar{Q}$=1.5 ; C) $\bar{Q}$=2

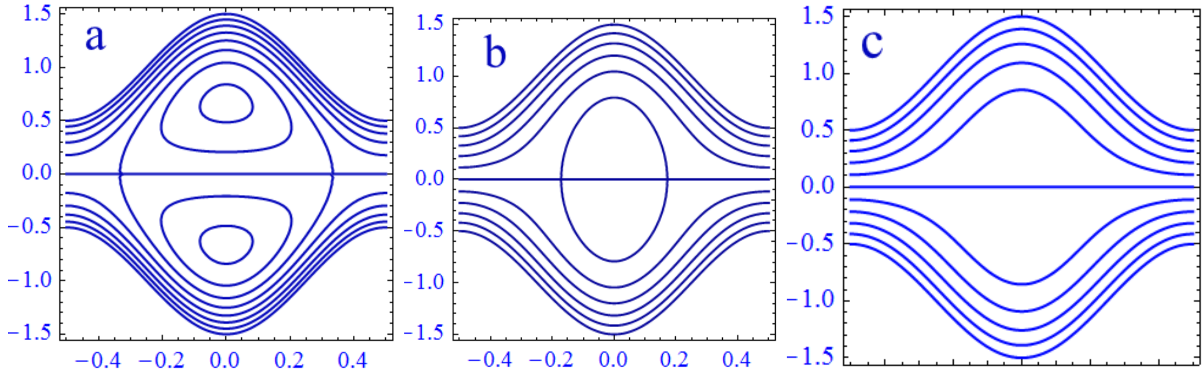

Figure 8: Streamlines for a=0.5, B=0.5, D=1, $\phi = 0$, $\bar{Q}$ =1.5 and for Different β ; A) $\beta = 0$; B) $\beta = 0.05$; C) $\beta = 0.1$

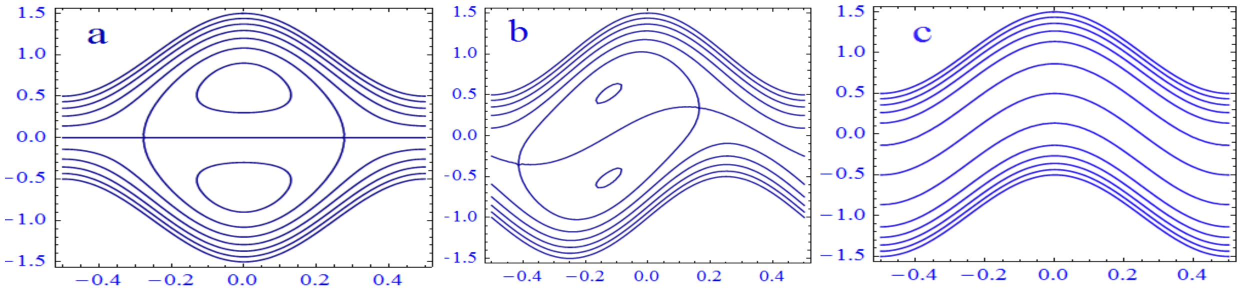

Figure 9: Streamlines for A=0.5, B=0.5, D=1, $\beta = 0.1$, $\bar{Q}$=1.5 and for Different ϕ ; A) $\phi = 0$; B) $\phi = \pi/2$; C) $\phi = \pi$

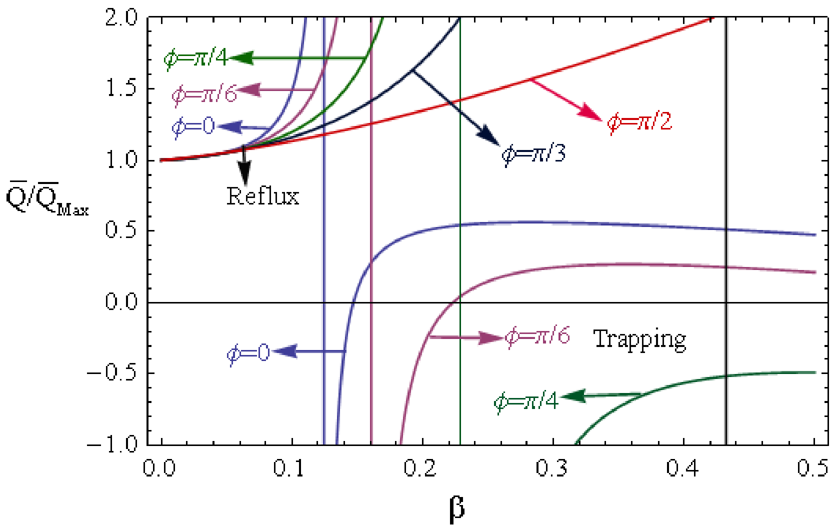

Figure 10: Trapping and Reflux Limit for Different ϕ with A=0.6, B=0.5, D=0.5 and $\Delta p = 0.6$

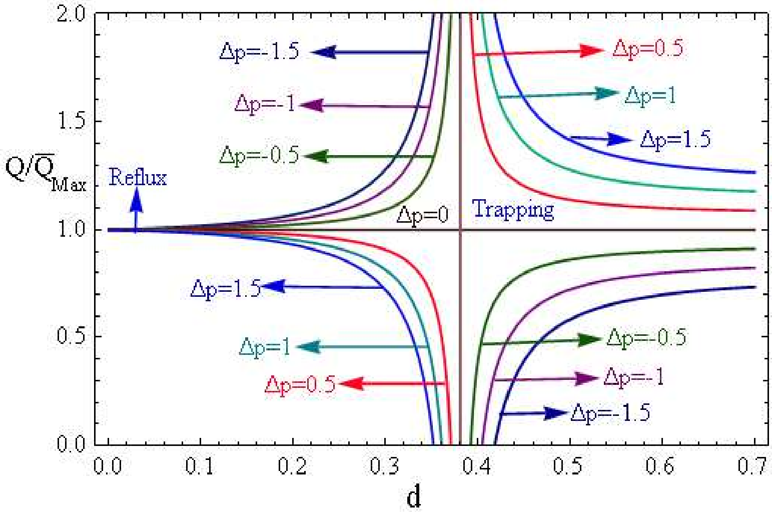

Figure 11: Trapping and Reflux Limit for Different d with A=0.6, B=0.5, $\phi = \pi/6$ and $\beta = 0.1$

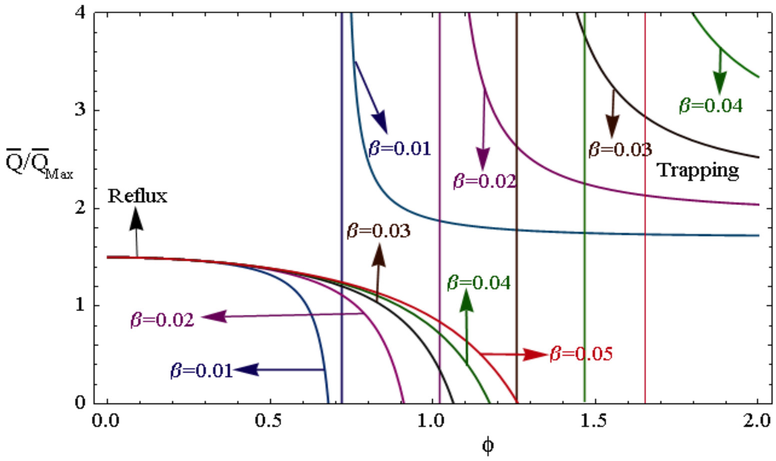

Figure 12: Trapping and Reflux Limit for Different d with A=1, B=0.5, D=0.5 and $\Delta p = 0.5$